

$\pi^-p$  scattering. — The same type of analysis starting with the  $I = \frac{3}{2}$  and  $I = \frac{1}{2}$  amplitudes leads to the differential cross sections

$$(d\sigma/dt)|_{\pi^+p\text{el}} \cong |a|^2 e^{\alpha t}, \quad (6a)$$

$$(d\sigma/dt)|_{\pi^-p\text{el}} \cong (|a|^2/9)e^{\alpha t} \{1 + 4|\eta \cos\gamma_0 + 4|\eta|^2\}, \quad (6b)$$

$$(d\sigma/dt)|_{\text{ce}} \cong (2|a|^2/9)e^{\alpha t} [1 - 2|\eta| \cos\gamma_0 + |\eta|^2 + 2|\eta| \sin\gamma_0 (\gamma_1 t + \gamma_2 t^2)] \\ \cong (C_0 - C_1 t - C_2 t^2) e^{\alpha t}. \quad (6c)$$

Again one can fit the data extremely well (Fig. 2) by the following choice of the parameters:

$$\alpha \cong 9, \quad |a|^2 = 30, \quad |\eta| \approx 1; \\ C_0 = 0.2, \quad C_1 = 2.3, \quad C_2 = 7.3.$$

The phase measurements of elastic and charge-exchange amplitudes given by Foley *et al.*<sup>8</sup> are not accurate enough to fix  $\gamma_0$ . If  $\gamma_0$  is known, one can again predict  $\varphi(t)$ , as in Eq. (5).

Thus we see that diffraction peaks in each isospin channel provide a natural explanation of the observed "anomaly" in the charge-exchange scattering. No spin-flip amplitude has been needed to fit the data up to  $t = -0.4$ . The spin-flip amplitude may play a role for larger values of  $t$  and cause the secondary peaks, as in the case of elastic scattering.<sup>7</sup> The measurements of relative phases and polarization will decide whether the present mechanism or the spin-flip hypothesis causes the near-forward peaks in charge-exchange scattering.

\*Work supported in part by the U. S. Air Force Office of Scientific Research under Grant No. AF-AFOSR-30-65.

<sup>1</sup>A. V. Sterling *et al.*, Phys. Rev. Letters **14**, 763 (1965).

<sup>2</sup>P. Astbury *et al.*, Phys. Letters **16**, 326 (1965).

<sup>3</sup>W. H. Fisher, Helv. Phys. Acta **38**, 629 (1965).

<sup>4</sup>N. Byers and C. N. Yang, Phys. Rev. **142**, 976 (1966).

<sup>5</sup>M. Barger and M. Ebel, Phys. Rev. **138**, B1148 (1965).

<sup>6</sup>P. Sonderegger *et al.*, Phys. Letters **20**, 75 (1966).

<sup>7</sup>A. O. Barut and W. S. Au, Phys. Rev. Letters **13**, 489 (1964).

<sup>8</sup>K. J. Foley *et al.*, Phys. Rev. Letters **14**, 862 (1965).

## EXCHANGE-DEGENERACY CLASSIFICATION OF REGGE TRAJECTORIES AND THE TOTAL CROSS SECTIONS\*

Akbar Ahmadzadeh

University of California, San Diego, La Jolla, California

(Received 11 April 1966)

In this Letter we present an analysis of the meson-nucleon, nucleon-nucleon, and nucleon-antinucleon total cross sections. The analysis is based on Regge trajectories whose factorized reduced residues are related by SU(3) symmetry. Thus, in this respect our treatment is basically the same as that of Barger and Olsson<sup>1</sup> but with some minor differences. Furthermore, we make the additional assumption of exchange degeneracy with respect to the signature as hypothesized by Arnold.<sup>2</sup> The trajectories to which we apply this hypothesis are, however, not exactly the same as those chosen by Arnold, and we assume that the residues, as well as the trajectory functions, exhibit this degeneracy. Our aim is to show that the experimental data on total cross sections are in agreement with

this hypothesis, thereby raising the possibility of reducing the number of parameters in Regge-pole phenomenology.

It can be shown,<sup>3</sup> under rather general assumptions, that the nucleon-nucleon and nucleon-antinucleon total cross sections depend only on the exchange of four sets of quantum numbers specified by vacuum,  $\rho$ ,  $\omega$ , and  $R$ . This is also the case for kaon-nucleon cross sections. For the pion-nucleon case, the exchange of the quantum numbers of  $\omega$  and  $R$  does not contribute due to the  $G$ -parity conservation. In the Regge-pole model these four types of exchanges are in the form of Regge trajectories. Note that there may be more than one trajectory for a given set of quantum numbers.

Now it is well known that the vector mesons

$[\rho(760), K^*(890), \varphi(1020), \omega(783)]$  form an SU(3) nonet with  $\omega$ - $\varphi$  mixing. Here we take the mixing angle to be such that the Gell-Mann-Okubo mass formula is exactly satisfied. Namely, we have

$$4m_{K^*}^2 = m_\rho^2 + 3m_{V_8}^2, \quad (1)$$

where  $V_8$  (and  $V_1$ ) are related to  $\omega$  and  $\varphi$  by the mixing angle  $\theta_V$ :

$$\begin{aligned} |V_8\rangle &= \cos\theta_V |\varphi\rangle + \sin\theta_V |\omega\rangle, \\ |V_1\rangle &= -\sin\theta_V |\varphi\rangle + \cos\theta_V |\omega\rangle. \end{aligned} \quad (2)$$

Thus, we find  $\cos\theta_V = 0.77$ ,  $m_{V_8}^2 = 0.86 \text{ BeV}^2$ ,  $m_{V_1}^2 = 0.79 \text{ BeV}^2$ . We associate each member of the octet ( $\rho, K^*, V_8$ ) and the singlet ( $V_1$ ) with a Regge trajectory—the same mass formula (1) being satisfied among the members of the octet of the trajectories at any fixed angular momentum  $J$ . In a manner similar to Barger and Olsson,<sup>1</sup> we take the SU(3)-symmetric interactions between the vector mesons and the pseudoscalar and baryon octets at the forward direction to be given by

$$\begin{aligned} L_{VMM} &= \sqrt{2}\gamma_M \langle M[V, M] \rangle, \\ L_{V\bar{B}B} &= \sqrt{2}\gamma_N (f\langle \bar{B}[V, B] \rangle + d\langle \bar{B}[V, B] \rangle) \\ &\quad + \sqrt{2}\eta_N V_1 \langle \bar{B}B \rangle, \end{aligned} \quad (3)$$

where  $\gamma_M$  and  $\gamma_N$  are the reduced factorized residues of the vector octet coupling to the mesons and nucleons, respectively, and  $\eta_N$  is the corresponding residue for the vector-meson singlet coupling to the baryons. Here  $M$ ,  $V$ , and  $B$  stand for the  $3 \times 3$  matrices for the appropriate octets as given by Ne'eman,<sup>4</sup> and  $\langle \rangle$  means the trace over the SU(3) indices. From (3) one finds

$$\begin{aligned} \frac{1}{2}\gamma_{\pi\rho} = \gamma_{K\rho} = \gamma_{KV_8}/\sqrt{3} = \gamma_M, \quad \gamma_{KV_1} = \gamma_{\pi V_1} = 0, \\ \gamma_{p\rho} = \gamma_N, \quad \gamma_{pV_8} = (3f-d)/\sqrt{3}\gamma_N, \quad \gamma_{pV_1} = \sqrt{2}\eta_N, \end{aligned} \quad (4)$$

where, for example,  $\gamma_{\pi\rho}$  stands for the factorized coupling of the  $\rho$  Regge pole at the forward direction and at the  $\rho\pi\pi$  vertex.

Similarly, the tensor mesons<sup>5</sup> [ $A_2(1310)$ ,  $K^{*'}(1430)$ ,  $s_0(1525)$ ,  $f_0(1250)$ ] are also expected to form a nonet. The  $A_2$  meson belongs to the  $R$  trajectory and was predicted by Pignotti<sup>6</sup> from the SU(3) symmetry and bootstrap dynam-

ics. The combination of the  $\rho$  and  $R$  trajectories was used by the present author<sup>7</sup> in an attempt to explain the  $n\bar{p}$  charge-exchange cross sections. Here we assume that the amount of singlet-octet mixing for the tensor mesons is again such that the mass formula is exactly satisfied. Namely,

$$4m_{K^{*'}}^2 = m_{A_2}^2 + 3m_{T_8}^2, \quad (5)$$

with

$$\begin{aligned} |T_8\rangle &= \cos\theta_T |s_0\rangle + \sin\theta_T |f_0\rangle, \\ |T_1\rangle &= -\sin\theta_T |s_0\rangle + \cos\theta_T |f_0\rangle. \end{aligned} \quad (6)$$

Here we find  $\cos\theta_T \approx 0.88$ ,  $m_{T_8}^2 \approx 2.15 \text{ BeV}^2$ ,  $m_{T_1}^2 = 1.73 \text{ BeV}^2$ . As pointed out by Arnold,<sup>2</sup> if we consider the mesons as bound states of  $\bar{B}B$  systems in a bootstrap picture, the exchange part of the forces due to the two baryon systems is expected to be weak. Drawing the analogy with the potential scattering case<sup>8</sup> would thus indicate that trajectories of opposite signature and  $G$  parity should be degenerate. (One can also consider  $\bar{q}q$  instead of  $\bar{B}B$  with a similar result.) Using these arguments, we expect that the trajectories associated with  $\rho$ ,  $K^*$ ,  $V_8$ , and  $V_1$  to be almost overlapping with the corresponding  $A_2$ ,  $K^{*'}$ ,  $T_8$ , and  $T_1$  trajectories, respectively. By the same reasoning we expect that (apart from the signature factors) the couplings  $\gamma_M$ ,  $\gamma_N$ , etc., for the vector and tensor cases should also coincide. A straight-line approximation to the trajectories together with the above degeneracy hypothesis also determines the trajectory intercepts. The  $\rho$ - $R$ ,  $K^*$ - $K^{*'}$ ,  $V_8$ - $T_8$ , and  $V_1$ - $T_1$  trajectories based on the straight-line approximation<sup>9</sup> are given in Fig. 1.

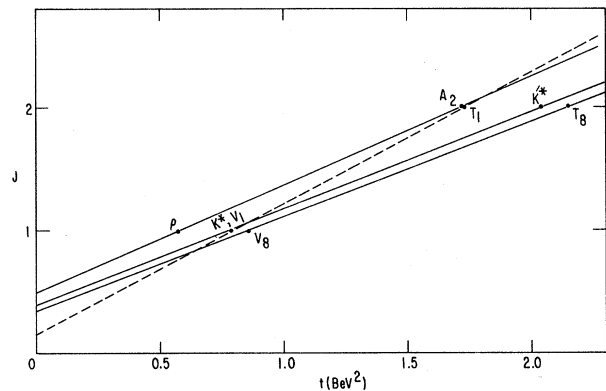


FIG. 1.  $\rho$ - $R$ ,  $K^*$ - $K^{*'}$ ,  $V_8$ - $T_8$ , and  $V_1$ - $T_1$  trajectories.

For the intercepts, at  $t=0$ , we find

$$\begin{aligned}\alpha_\rho = \alpha_R \simeq 0.5, \quad \alpha_{K^*} = \alpha_{K^{*'}} \simeq 0.35, \\ \alpha_{V_8} = \alpha_{T_8} \simeq 0.30, \quad \alpha_{T_1} = \alpha_{V_1} \simeq 0.15.\end{aligned}\quad (7)$$

Let us observe that the equality of intercepts and couplings of  $\rho$  and  $R$  implies equality of  $pp$  and  $pn$  total cross sections. This equality would be expected to hold even independent of SU(3) and is in reasonable agreement with the high-energy data.

Now in a manner similar to the vector meson case one can write the interactions to be of the form

$$\begin{aligned}L_{TMM} &= \sqrt{2}\gamma_M \langle M\{T, M\} \rangle + \sqrt{2}\eta_M T_1 \langle MM \rangle, \\ L_{T\bar{B}B} &= \sqrt{2}\gamma_N (f\langle \bar{B}\{T, B\} \rangle + d\langle \bar{B}\{T, B\} \rangle) \\ &\quad + \sqrt{2}\eta_N T_1 \langle \bar{B}B \rangle,\end{aligned}\quad (8)$$

from which we find

$$\begin{aligned}\gamma_{KR} &= \frac{1}{2}\sqrt{3}\gamma_{\pi T_8} = -\sqrt{3}\gamma_{KT_8} = \gamma_M, \\ \gamma_{KT_1} &= \gamma_{\pi T_1} = \sqrt{2}\eta_M, \quad \gamma_{pR} = \gamma_N, \\ \gamma_{pT_8} &= 3^{-1/2}(3f-d)\gamma_N, \quad \gamma_{pT_1} = \sqrt{2}\eta_N.\end{aligned}\quad (9)$$

In addition to the above, we use the Pomeron trajectory with intercept  $\alpha_p = 1$  and with couplings  $\Gamma_\pi$ ,  $\Gamma_K$ , and  $\Gamma_N$  in the same manner as Barger and Olsson.<sup>1</sup> Note that there can be no contribution from any trajectories with quantum numbers other than what we have considered.

Now with the trajectory intercepts known from Eqs. (7) we are left with eight parameters ( $\Gamma_\pi$ ,  $\Gamma_K$ ,  $\Gamma_N$ ,  $\gamma_M$ ,  $\gamma_N$ ,  $\eta_M$ ,  $\eta_N$ , and  $f/d$ ) which are fitted to the experimental data on the cross sections. In terms of these parameters the total cross sections are given by

$$\begin{aligned}\sigma_{\pi-p} &= 2\Gamma_\pi \Gamma_N R_{\pi P} + \frac{2}{3}(4f-1)\gamma_M \gamma_N R_{\pi 8} \\ &\quad + 2\gamma_M \gamma_N R_{\pi \rho} + 2\eta_M \eta_N R_{\pi 1}, \\ \sigma_{\pi+p} &= 2\Gamma_\pi \Gamma_N R_{\pi P} + \frac{2}{3}(4f-1)\gamma_M \gamma_N R_{\pi 8} \\ &\quad - 2\gamma_M \gamma_N R_{\pi \rho} + 2\eta_M \eta_N R_{\pi 1}, \\ \sigma_{K-p} &= 2\Gamma_K \Gamma_N R_{KP} + \frac{2}{3}(4f-1)\gamma_M \gamma_N R_{K 8} \\ &\quad + 2\gamma_M \gamma_N R_{K \rho} + 2\eta_M \eta_N R_{K 1},\end{aligned}$$

$$\begin{aligned}\sigma_{K+p} &= 2\Gamma_K \Gamma_N R_{KP} - \frac{4}{3}(4f-1)\gamma_M \gamma_N R_{K 8} \\ &\quad + 2\eta_M \eta_N R_{K 1}, \\ \sigma_{K-n} &= 2\Gamma_K \Gamma_N R_{KP} + \frac{2}{3}(4f-1)\gamma_M \gamma_N R_{K 8} \\ &\quad - 2\gamma_M \gamma_N R_{K \rho} + 2\eta_M \eta_N R_{K 1}, \\ \sigma_{K+n} &= 2\Gamma_K \Gamma_N R_{KP} - \frac{4}{3}(4f-1)\gamma_M \gamma_N R_{K 8} \\ &\quad + 2\eta_M \eta_N R_{K 1}, \\ \sigma_{\bar{p}p} &= 2\Gamma_N^2 R_{NP} + \frac{2}{3}(4f-1)^2 \gamma_N^2 R_{N 8} \\ &\quad + 2\gamma_N^2 R_{N \rho} + 4\eta_N^2 R_{N 1}, \\ \sigma_{pp} &= 2\Gamma_N^2 R_{NP}, \\ \sigma_{pn} &= 2\Gamma_N^2 R_{NP} + \frac{2}{3}(4f-1)^2 \gamma_N^2 R_{N 8} \\ &\quad - 2\gamma_N^2 R_{N \rho} + 4\eta_N^2 R_{N 1}, \\ \sigma_{pn} &= 2\Gamma_N^2 R_{NP}.\end{aligned}\quad (10)$$

Note that the above formulas imply  $\sigma_{pp} = \sigma_{pn} \simeq \text{constant}$  and  $\sigma_{K+p} = \sigma_{K+n}$  in reasonable agreement with the experimental data. In Eq. (10) we have used  $f+d=1$ ; and, for example,  $R_{\pi\rho}$  is given by

$$R_{\pi\rho} = \frac{\pi^{1/2}}{s^{1/2}q_{\pi N}} \frac{\Gamma(\alpha_\rho + \frac{3}{2})}{\Gamma(\alpha_\rho + 1)} \left[ \frac{s - m_\pi^2 - m_N^2}{s_0} \right]^{\alpha_\rho}, \quad (11)$$

where we take, as usual,  $s_0 = 1 \text{ BeV}^2$ ; and in terms of the laboratory momentum of the incident particle (the pion, in this example), we have

$$s^{1/2}q_{\pi N} = p_\pi m_N$$

and

$$s - m_\pi^2 - m_N^2 = 2m_N(p_\pi^2 + m_\pi^2)^{1/2}.$$

The experimental data<sup>10</sup> and the theoretical curves from fitting the eight parameters are given in Fig. 2. The numerical values of the parameters and their estimated errors are

$$\begin{aligned}\Gamma_\pi &= 2.87 \pm 0.02, \quad \Gamma_K = 2.22 \pm 0.02, \\ \Gamma_N &= 4.94 \pm 0.02, \quad \gamma_M = 1.10 \pm 0.07, \\ \gamma_N &= 1.18 \pm 0.09, \quad f/d = -1.90 \pm 0.1, \\ \eta_M &= 2.90 \pm 1.0, \quad \eta_N = 2.17 \pm 0.8.\end{aligned}\quad (12)$$

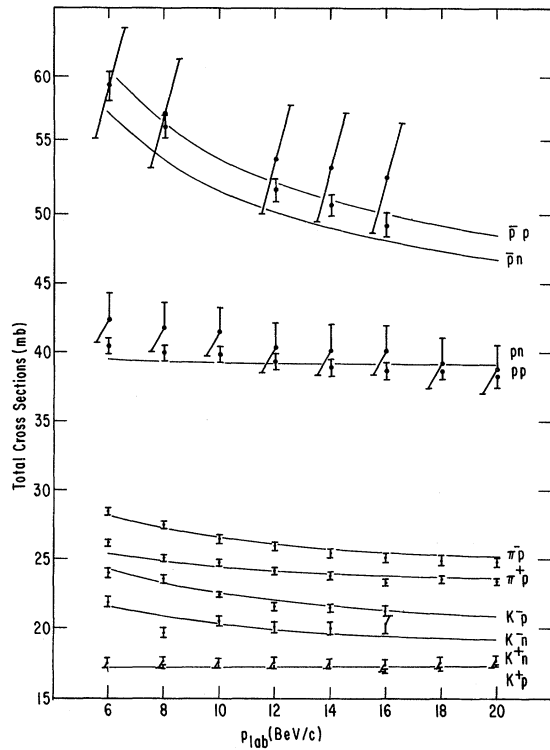


FIG. 2. Experimental data on total cross sections and the theoretical curves from fitting the parameters as described in the text.

The chi-squared value obtained here is  $\chi^2 = 75$  for 70 data points fitting eight parameters. This can be compared with the calculations of Barger and Olsson<sup>1</sup> who obtain  $\chi^2 = 61$  for 93 data points fitting 14 parameters.

Let us now make the following remarks: (i) We need not speculate here about the values of the couplings  $\gamma$  away from the forward direction. However, if we require the couplings to be degenerate also for negative  $t$  values, then one would expect that the vector (as well as the tensor) residues should have "ghost-killing" factors. It is well known that the residues fall off rapidly with negative  $t$ . The exact vanishing of the vector-trajectory residues is, however, not really required because the exchange degeneracy is, after all, not exact. (ii) We have taken the same  $\gamma_M$  in Eqs. (3) and (8).

Removal of this condition would merely introduce one more parameter.

To summarize, we have shown that the experimental data on the high-energy total cross sections are in reasonable agreement with the exchange degeneracy of the trajectories. This hypothesis reduces the number of parameters. One can use the parameters obtained here to calculate other relevant quantities as a further check for the validity of the above hypothesis. Finally, let us point out that we have here associated no known resonance with the Pomeron-chuck trajectory. There have been recent arguments that there may be a resonance of the desired quantum numbers near the  $\rho$  mass.<sup>11,12</sup>

\*Work supported in part by the U. S. Atomic Energy Commission.

<sup>1</sup>V. Barger and M. Olsson, Phys. Rev. Letters **15**, 930 (1965); also to be published. For the numerous references to the recent phenomenological calculations based on Regge poles see R. J. N. Phillips and W. Rarita, Phys. Rev. **139**, B1336 (1965).

<sup>2</sup>Richard C. Arnold, Phys. Rev. Letters **14**, 657 (1965).

<sup>3</sup>Akbar Ahmadzadeh and Elliot Leader, Phys. Rev. **134**, B1058 (1964).

<sup>4</sup>Y. Ne'eman, Nucl. Phys. **26**, 222 (1961).

<sup>5</sup>S. L. Glashow and R. H. Socolow, Phys. Rev. Letters **15**, 329 (1965).

<sup>6</sup>A. Pignotti, Phys. Rev. **134**, B630 (1964).

<sup>7</sup>A. Ahmadzadeh, Phys. Rev. **134**, B633 (1964).

<sup>8</sup>S. C. Frautschi, M. Gell-Mann, and F. Zachariasen, Phys. Rev. **126**, 2204 (1962).

<sup>9</sup>In fact, the trajectories do have a curvature, and it would be interesting to obtain a phenomenological  $\rho$ - $R$  trajectory using the experimental data of masses and widths, etc., of  $\rho$  and  $A_2$  mesons. In so doing, the intercepts would be slightly different from the straight-line case used here. We can apply the previous method [see A. Ahmadzadeh and I. Sakmar, Phys. Rev. **133**, B1290 (1964)] to find a better estimate of the  $\rho$ - $R$  trajectory.

<sup>10</sup>For a list of references to the experimental data, see Barger and Olsson, Ref. 1.

<sup>11</sup>B. R. Desai, "The existence of a  $2^+$  Unitary Singlet Near the  $\rho$ -Meson Mass" (to be published). Also, H. Munczek, A. Pignotti, and M. A. Virasoro, Phys. Rev. **145**, 1154 (1966).

<sup>12</sup>Bipin R. Desai and Peter G. O. Freund, Phys. Rev. Letters **16**, 622 (1966).